

## Advances in III-Nitride Microstructures and Micro-Size Emitters

H. X. JIANG\* and J. Y. LIN

*Department of Physics, Kansas State University, Manhattan, KS 66506-2601, U.S.A.*

This paper summarizes some of the recent advances in III-nitride microstructures and micro-size emitters made by the author's group. Microstructures discussed include micro-size disk, ring, and pyramid structures. Optical mode behaviors in these microcavities were probed by optical pumping and measuring the photoluminescence (PL) emission from individual cavities. It was found that the microdisk cavities support both the Whispering Gallery (WG) and the radial modes, while the microring cavities support only the WG type. Micro-size pyramids were also obtained by selective epitaxial overgrowth. It was shown that these pyramids are highly efficient resonators and each pyramidal microcavity is a true 3-D cavity that can support more than three different groups of optical resonance modes. The current injected micro-size LEDs were successfully fabricated from InGaN/GaN quantum wells. It was found that quantum efficiencies in these micro-size LEDs were significantly greater than in conventional broad-area LEDs. A novel light emitting diode (LED) architecture based on interconnecting hundreds of microdisk LEDs was successfully fabricated. It was demonstrated that the emission efficiency was boosted by as much as 50 % in this novel device. The operation of an individually addressable III-nitride microdisk LED array or the first prototype semiconductor microdisplay was also demonstrated. The III-nitride microdisplay can potentially provide unsurpassed performance over those based on the liquid crystal or organic LED technologies. Some of the future trends and challenges facing the III-nitride microcavity photonic devices are also discussed.

PACS numbers: 72.80.Ey, 73.40.Kp, 73.40.Lq

Keywords: III-Nitrides, Microcavities, Micro-size emitters, Photonics

### I. INTRODUCTION

III-nitrides have recently attracted considerable interest due to their applications for optical devices that are active in the blue and ultraviolet (UV) wavelength regions and electronic devices capable of operation at high temperatures/power levels, and in harsh environments. Researchers in this field have made extremely rapid progress toward materials growth as well as device fabrication [1–6]. The successes of super-bright blue light emitting diodes (LED) and laser diodes (LDs) based on the III-nitride system are a clear indicative of the great potential of this material system. The recent success of the III-nitride edge-emitters, including blue LEDs and LDs, is encouraging for the study of microcavity laser diodes (MCLDs), microcavity LEDs (MCLEDs), and micro-LEDs. New physical phenomena and properties begin to dominate as the device size scale approaches the wavelength of light, including modified spontaneous emission, enhanced quantum efficiency, and lasing in microcavities, all of which warrant fundamental investigations [7, 8]. The micro-size light emitting devices offer benefits over edge-emitters including the ability to create arrays of individually controllable pixels on a single

chip, enhanced quantum efficiency, and greatly reduced lasing threshold.

We have fabricated arrays of microstructures from GaN/AlGaIn and InGaIn/GaN multiple quantum well (MQW) with dimension from 2 to 20  $\mu\text{m}$  [9–12]. Photo- and e-beam lithography and inductively coupled plasma (ICP) etching were employed to pattern the microstructures. Optical properties have been studied. The intrinsic transitions from the well regions were found to exhibit an approximate 10-fold increase in both recombination lifetime and quantum efficiency upon formation of microstructures. Our results on GaN/AlGaIn and InGaIn/GaN MQW microdisk and microring cavities show that when an individual disk or ring is optically pumped, resonance modes corresponding to the radial and the whispering-gallery (WG) modes are simultaneously present in microdisk cavities, but only WG modes are available from the microring cavities. Our results have also indicated that the carrier dynamic processes in QW microstructures are quite different than those in QWs.

We have also studied optical properties of GaN hexagonal micro-pyramid arrays with smooth facets obtained by selective epitaxial overgrowth [13, 14]. These self-organized pyramids are highly efficient microresonators. Optical resonance modes in the self-organized pyramid resonators were observed at a pumping intensity which

---

\*E-mail: jiang@phys.ksu.edu

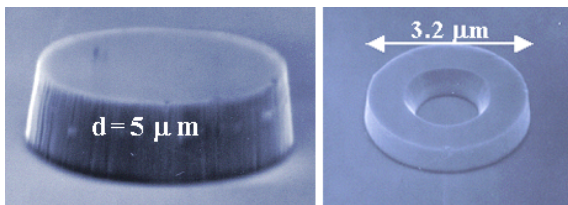


Fig. 1. SEM images of different III-nitride microstructures fabricated by photolithography patterning and inductively coupled plasma dry etching [after Ref. 12].

is several orders of magnitude lower than that required in the InGaN/GaN and GaN/AlGaIn MQW microdisk cavities fabricated by dry etching [14].

Recently our research group has successfully fabricated electrically-pumped individual III-nitride micro-size LEDs and micro-LED arrays and observed enhanced quantum efficiencies [15]. Applications of these micro-size LEDs have also been explored. Two examples discussed include III-nitride interconnected micro-size LEDs for boosting LED emission efficiencies and microdisplays [16,17].

## II. EXPERIMENT

The III-nitride microdisks and microrings used in our studies were prepared from MQW structures, which were grown on (0001) sapphire substrates. The GaN/AlGaIn MQW samples were grown either by metal organic chemical vapor deposition (MOCVD) or reactive molecular beam epitaxy (MBE) and consists of a 50 nm AlN buffer layer followed by a 10 period 50 Å/50 Å GaN/Al<sub>x</sub>Ga<sub>1-x</sub>N ( $x \sim 0.07$ ) MQW and a 200 Å AlN cap layer. The InGaIn/GaN MQW was grown by MOCVD and consists of a 50 nm GaN buffer layer followed by a 20 period 45 Å/45 Å In<sub>x</sub>Ga<sub>1-x</sub>N/GaN ( $x \sim 0.15$ ) MQW. All layers were grown nominally undoped. Photolithography and ICP dry etching was used to pattern arrays of microdisks and microrings with varying diameters and separation spacings. The samples were etched into the sapphire substrate so that no III-nitride material is present between microstructure. Figures 1 shows the scanning electron microscopy (SEM) images of representative III-nitride microstructures prepared by ICP etching.

GaN micropyramids were obtained by selective epitaxy overgrowth on the GaN epilayers on sapphire or silicon substrates using MOCVD. Before the pyramidal overgrowth, a 1-μm-thick GaN epilayer was grown on a (0001) sapphire or silicon substrate with a thin AlN buffer layer. A 0.2-μm-thick SiO<sub>2</sub> mask was coated on the GaN epilayer. Hexagonal or circular windows on the SiO<sub>2</sub> mask were prepared by photolithography together with dry etching followed by the GaN pyramidal overgrowth. These GaN pyramids formed a 2D array.

The micro-size LEDs were fabricated from LED wafers

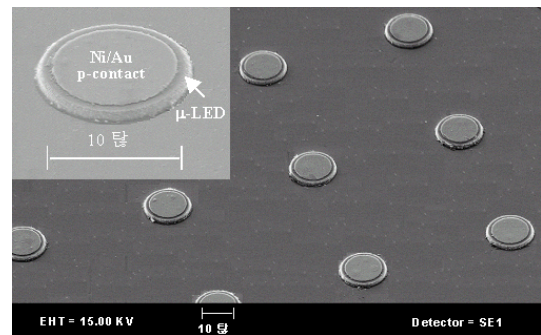


Fig. 2. SEM image of a III-nitride microdisk LED array fabricated by photolithography patterning, inductively coupled plasma dry etching, and Ohmic contact metallization [after Ref. 15].

based on the InGaIn/GaN QW structure. Our LED structures were grown on sapphire substrates with 30 nm GaN buffer layers. The QW device layers comprise 3.5 μm of Si-doped GaN, 0.1 μm of silicon doped superlattice consisting alternating layers of 50 Å /50 Å of AlGaIn/GaN, a 50 Å of silicon doped GaN, 20 Å undoped InGaIn active layer, 0.14 μm of Mg doped superlattice consisting alternating layers of 50 Å/50 Å of AlGaIn/GaN, and 0.5 μm Mg-doped GaN epilayer, followed by a rapid thermal anneal at 950 °C for 5 seconds in nitrogen. This process produced p-layer concentrations of  $5 \times 10^{17}$  (hole mobility 12 cm<sup>2</sup>/Vs) and n-layer concentrations of  $1.6 \times 10^{18}$  (electron mobility 310 cm<sup>2</sup>/Vs). By incorporating the AlGaIn/GaN superlattice structure into our LED device layers, the p-type concentration was enhanced from  $2 \times 10^{17}$  to  $5 \times 10^{17}$  cm<sup>-3</sup>. Microdisk LED arrays such as that shown in Fig. 2 with individual micro-LED size varying from 5 to 20 μm were fabricated by photolithographic patterning and inductively coupled plasma (ICP) dry etching. Bilayers of Ni (20 nm)/Au (200 nm) and Al (300 nm)/Ti (20 nm) were deposited by electron beam evaporation as p- and n-type Ohmic contacts. The p- and n-type contacts were thermally annealed in nitrogen ambient for 5 min at 650 °C. The emission wavelengths of our micro-size LEDs vary from green to purple (390 to 450 nm) by varying In content in the InGaIn active layers.

For photoluminescence (PL) studies, UV excitation pulses with pulse width of about 7 ps at a repetition rate of 9.5 MHz were provided by a picosecond UV laser system which consists of a Yttrium-Aluminum-Garnet (YAG) laser (Coherent Antares 76) with a frequency doubler which pumps a cavity-dumped dye laser (coherent 702-2CD) with Rhodamine 6G dye solution and a second frequency doubler after the dye laser to provide a tunable photon energy up to 4.5 eV. The laser output after the second doubler has an average power of about 30 mW and a spectral width of about 0.2 meV. The excitation intensity was controlled by a set of UV neutral density filters. Two detection systems were used

to record the PL. A single photon counting detection system with a microchannel-plate photomultiplier tube (MCP-PMT) has a time-resolution of about 25 ps. A streak camera (Hamamatsu-C5680) detector has a time-resolution of about 2 ps [18].

To study the resonance modes behaviors, an UV transmitting objective was used in a confocal geometry to optically pump a single microstructure normal to the sample surface and to collect the light emission in the direction of the surface normal. Focused beam spot diameters as small as 2  $\mu\text{m}$  could be achieved with the objective lens.

### III. RESULTS AND DISCUSSIONS

#### 1. III-nitride microdisks

Optical resonance modes are observed in individually pumped microdisks under high pump intensity. The description of optical resonance modes in a thin dielectric disk involves the satisfaction of Maxwell's equations across a boundary of cylindrical symmetry [19–21]. The fields within the disk are described by Bessel functions while the evanescent wave outside of the disk is described by Hankel functions. It has been pointed out that the microdisk cavity may support two distinctly different resonant mode types [21]. One mode type is described by Bessel functions  $J_m(\chi)$  with  $m = -1, 0, 1$  within the cavity. These modes are dominated by photon wave motion along the radial direction of the disks. The equivalent optical path is formed between the edge and the center of the disk giving an effective round-trip cavity length of  $2R$  where  $R$  is the radius of the microdisk. This mode consists of radial oscillations of field intensity much like the wavelets formed by a pebble dropped in still water. Another type, known as the Whispering Gallery (WG) mode [22], is described by Bessel functions  $J_m(\chi)$  for large  $m$ . The WG mode may be thought of as in-plane propagation around the inside perimeter of the disk which is facilitated by total-internal-reflection. An effective optical path of  $2\pi Rn$  is given by the periodic boundary condition imposed on the circulating wave with  $n$  being the index of refraction of the microdisk.

Strong optical mode behavior is observed in the emission spectra of individually pumped InGaN/GaN MQW microdisks as shown in Fig. 3(a). These mode peaks may be compared with the emission spectrum shown in Fig. 3(b) from the InGaN/GaN MQWs without microdisks obtained under equivalent conditions.

The three small peaks (3.304 eV, 3.312 eV, 3.320 eV) seen at the high energy side of Fig. 3(a) exhibit spacing of 8 meV and are attributed to alternating TE and TM WG modes. The labeled peaks on the low energy side of the spectrum (3.174 eV, 3.181 eV, 3.188 eV, 3.195 eV) are separated by 7 meV and also attributed to the WG mode. The three large peaks (3.219 eV, 3.244 eV, 3.271 eV)

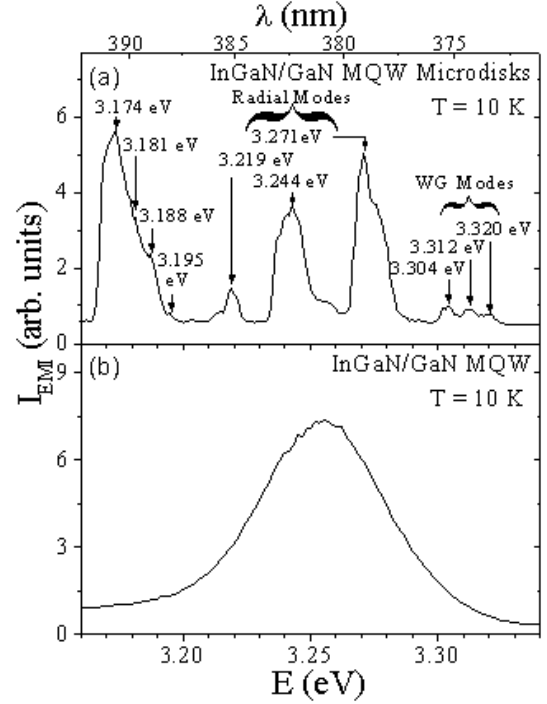


Fig. 3. Emission spectrum of (a) an individually pumped InGaN/GaN MQW microdisk and (b) the InGaN/GaN MQW without microdisks. Optical modes of the whispering-gallery (WG) and radial type were observed in (a). The observed mode spacings were consistent with calculation results [after Refs 9-11].

eV), on the other hand, are spaced by approximately 26 meV and due to alternating TE and TM radial ( $m = 0$ ) modes. The spacing and assignment of the two mode types are discussed in more detail in the following.

We assume the disk walls are perfectly conducting so that the field outside of the disk vanishes. In this way, approximate mode positions and spacings are readily derivable. For the radial mode type ( $m = 0$ ), the fields within the disk are described by zeroth order Bessel functions and the boundary condition for a TM (TE) mode requires that  $J_0(kR) = 0$  [or  $J_0'(kR) = 0$ ]. Here,  $k$  is the photon wave number in the disk and  $k = 2\pi/(\lambda/n)$  with  $\lambda$  being the wavelength of the mode. Differentiation is performed with respect to the radial variable. For the case of  $m = 0$ , the optical modes can be found by noting that in the limit of  $kR \gg 1$  (as in this case),

$$J_0(kR) \approx (2/\pi kR)^{1/2} \cos(kR - \pi/4) \quad (1)$$

We can thus obtain the eigenmodes for the case  $m=0$  as  $J_0(kR) = 0$  ( $J_0'(kR) = 0$ ), or equivalently,

$$\text{TM modes : } 2nR = (p + 3/4)\lambda, p = 1, 2, 3 \dots \quad (2)$$

$$\text{TE modes : } 2nR = (p + 1/4)\lambda, p = 1, 2, 3 \dots \quad (3)$$

From Eqs. (2) and (3), we find both the TE and TM radial modes exhibit a mode spacing of

$$\Delta\lambda_{rad}^{TE} = \Delta\lambda_{rad}^{TM} = \lambda^2/2Rn \quad (4)$$

The second type of microdisk cavity mode is the WG mode. This mode has a low loss due to the total-internal-reflection and thus low threshold for lasing. The effective optical path length of  $2\pi Rn$  imposed by the periodic boundary condition results in a WG eigenmode condition of

$$2\pi Rn = m\lambda, \quad \text{for large(integer)}m \quad (5)$$

and the mode spacing is given by

$$\Delta\lambda_{WG} = \lambda^2/2\pi Rn = \Delta\lambda_{rad}/\pi \quad (6)$$

It is shown in Eq. (6) that the radial mode spacing is expected to be larger than the WG mode spacing by a factor of  $\pi$ . For the InGaN/GaN MQW microdisk emission spectrum shown in Fig. 3(a), mode spacings of 16 meV and 52 meV are observed (TE to TE or TM to TM). Calculation of the expected spacings with Eqs. (4) and (6) and representative values of  $R = 4.65 \mu\text{m}$  and  $n = 2.6$  reveals that the observed spacings correspond well to the WG and radial mode types, respectively. From the observed mode spacings of 16 meV and 52 meV for the WG and the radial modes, we indeed obtain the ratio of  $\Delta\lambda_{rad}/\Delta\lambda_{WG} = 3.25 \approx \pi$  as expected from Eq. (6).

## 2. III-nitride microrings

We have also fabricated and studied an InGaN/GaN MQW microring array. A PL emission spectrum obtained at 10 K from the InGaN/GaN MQWs prior to the microring fabrication is plotted in Fig. 4 (a), where the emission line at 3.470 eV is originated from the GaN barriers. The emission line at 3.288 eV is originated from the InGaN wells. The emission lines at 3.198 eV and 3.108 eV are the one and two phonon replicas of the 3.288 eV emission line. An emission spectrum measured at 10 K under high pumping intensity for an individually pumped InGaN/GaN MQW microring with an inner diameter of  $3.2 \mu\text{m}$  and a ring width of  $0.7 \mu\text{m}$  is shown in Fig. 4(b), where strong optical mode behavior is observed. Three strong emission lines at 3.116 eV, 3.170 eV, and 3.224 eV exhibiting a mode spacing of 54 meV are attributed to WG modes. The mode spacing of the WG modes is given by Eq. (6),  $\Delta\lambda_{WG} = \lambda^2/2\pi Rn$ , or by

$$\Delta E_{WG} = hc/2\pi Rn \quad (7)$$

in the energy spectrum, where  $h$  is the Planck constant,  $R$  is the radius of the ring,  $n$  is the index of refraction of the InGaN microrings, and  $\lambda$  is the wavelength of light propagating inside the ring cavity.

Calculated mode spacing for  $R = 1.6 \mu\text{m}$  and  $n = 2.6$  [23] is  $\Delta\lambda_{WG} = 60 \text{ \AA}$  (at  $\lambda = 3950 \text{ \AA}$ ) and  $\Delta\lambda_{WG} = 50 \text{ meV}$ , which agrees well with the observed mode spacing. The three peaks at 3.392 eV, 3.444 eV, and 3.494 eV in the high emission energy region, exhibiting

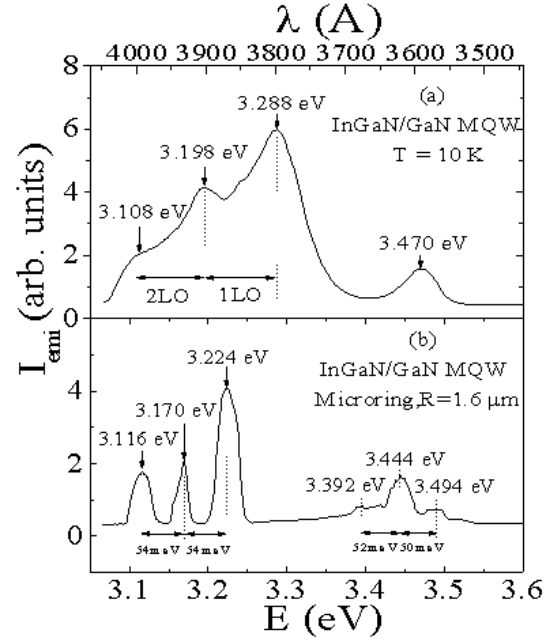


Fig. 4. Emission spectrum of (a) the InGaN/GaN MQW without microrings and (b) an individually pumped InGaN/GaN MQW microring. Optical modes of the whispering-gallery (WG) type were observed in (b). The observed mode spacings were consistent with calculation results [after Ref. 12].

a mode spacing of 52 meV and 50 meV, are also WG modes. The full width at half maximum (FWHM) of the resonance peaks is between 20 to 28 meV, which is attributed to the finite width of the microring as well as to the imperfection of the ring walls. The FWHM of the resonant modes can be calculated by

$$|\Delta(\Delta\lambda_{WG})| = (\lambda^2/2\pi R^2n)\Delta R = (\Delta R/R)\Delta\lambda_{WG}. \quad (8)$$

In the energy spectrum, the FWHM is given by

$$\Delta(\Delta E_{WG}) = \Delta[(hc/\lambda^2)\Delta\lambda_{WG}] = (\Delta R/R)\Delta E_{WG} \quad (9)$$

The calculated FWHM of the WG resonance modes from Eq. (9) is  $(\Delta R/R)\Delta E_{WG} = (0.7/1.6) \times 54 \approx 24 \text{ meV}$ , which agrees well with the value of 20 to 28 meV seen in Fig. 4(b).

The results for an individually pumped InGaN/GaN MQW microring can be compared with the InGaN/GaN MQW microdisk result shown in Fig. 3(a). For MQW microdisks, both the radial and the WG modes were observed with two distinct mode spacings and the ratio between the radial and the WG mode spacing is  $\pi$ . However, the WG mode is the only type of mode expected from a microring cavity [12]. Furthermore, the FWHM of the modes observed from the microring is much wider than that from the microdisk mainly due to the finite width of the ring. Unique features of WG modes in a microring cavity include that high Q values can be obtained relatively easily even in a very small mode volume

and the number of modes contributing to lasing can be reduced [24].

### 3. III-nitride micropyramids

III-nitride microstructures can also be obtained by selective epitaxial overgrowth using patterned GaN substrates. Selective epitaxial overgrowth has the advantage that photonic structures can be fabricated without process damage. It has been shown that GaN microcavities produced by selective epitaxial overgrowth using hexagonal or circular SiO<sub>2</sub> windows were of either hexagonal prisms or hexagonal pyramids due to the nature of the crystal structures of GaN [24–31]. Figure 5(a) shows a SEM image of a GaN micropyramid array fabricated by selective epitaxial overgrowth on GaN epilayers on sapphire substrate, which revealed that all six surfaces were extremely smooth. Prior to micro-pyramid formation, hexagonal or circular SiO<sub>2</sub> windows with size of about 3.5  $\mu\text{m}$  and 20  $\mu\text{m}$  apart were prepared by photolithography together with dry etching, followed by the GaN pyramidal overgrowth. Optical resonance modes were observed in individually pumped pyramids grown on sapphire substrates at a pumping intensity which is several orders of magnitude lower than that required in the InGaN/GaN and GaN/AlGaIn MQW microdisk cavities fabricated by dry etching [14]. Furthermore, as demonstrated in Fig. 5(b), the linewidth of the resonant modes seen in selectively overgrown pyramids is also narrower than those seen in microdisk or microring cavities fabricated by dry etching (*e.g.*, Fig. 3). Our results suggest that self-organized microcavities formed by selective epitaxy overgrowth can be further developed for the realization of GaN microcavity light emitters with high quality facets and hence minimum parasitic optical losses as well as a simplified device process that may eliminate the need of etching the crystal. We have shown that each pyramidal microcavity is a true 3D cavity that can support more than three different groups of optical resonance modes [14].

The selectively overgrown III-nitride microstructures could potentially be used for the development of two-dimensional laser arrays. Optically pumped laser action has already been achieved in GaN pyramids grown on (111) Si by selective lateral overgrowth of MOCVD [32].

### 4. Micro-size LEDs for boosting emission efficiencies

Bright blue LEDs based on III-nitrides paved the way for full color displays and raised the possibility of mixing three primary colors to obtain white light for general illumination by semiconductor LEDs. If all household 100 W light bulbs are replaced by white LEDs, the total energy savings in the World would approach \$ 100

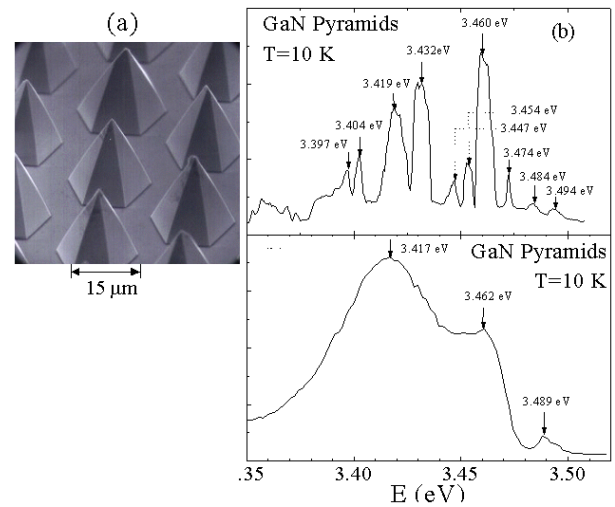


Fig. 5. SEM images of a self-organized III-nitride micropyramid array fabricated by selective-area over-growth. (b) Optical resonance modes in an individually pumped GaN pyramidal microcavity and (b) PL spectrum of a GaN pyramid array obtained under a low excitation condition [after Refs. 13 & 14].

billions/year. The associated reduction in environmental pollution can also be enormous. The current main approach for achieving white light using LEDs is to use phosphors to down-convert the emission from a blue or UV LED. In such an application, improving the LED efficiency is a key issue.

We have succeeded in interconnecting hundreds of III-nitride micro-size LEDs (size on the order of 10  $\mu\text{m}$  in diameter) [16]. As illustrated in Fig. 6, these microdisk LEDs are interconnected in a manner that they are turned on and off simultaneously and fit into the same device area taken up by a conventional LED of about  $300 \times 300 \mu\text{m}^2$ . The performance characteristics of the novel devices were compared with those of the conventional LEDs fabricated from the same LED wafers. It was shown that, the interconnected microdisk LEDs could boost the overall emission efficiency by as much as 50 %. It is believed that the novel device can overcome two biggest problems facing LEDs - the low extraction efficiencies due to the total internal reflection occurring at the LED/air interface and the problem of current spreading. Additionally, the strain induced piezoelectric field in the active QW regions may be reduced in micro-size LEDs, resulting in increased internal quantum efficiency. Furthermore, the processing steps of these interconnected micro-size LEDs are the same as those of the conventional LEDs. It is thus expected the manufacture yield of these novel LEDs to rival with the conventional LEDs. Currently, our group is working on the optimal configuration of this novel LED architecture, including the size of micro-LEDs, the spacing between the micro-LEDs, and the etching depth.

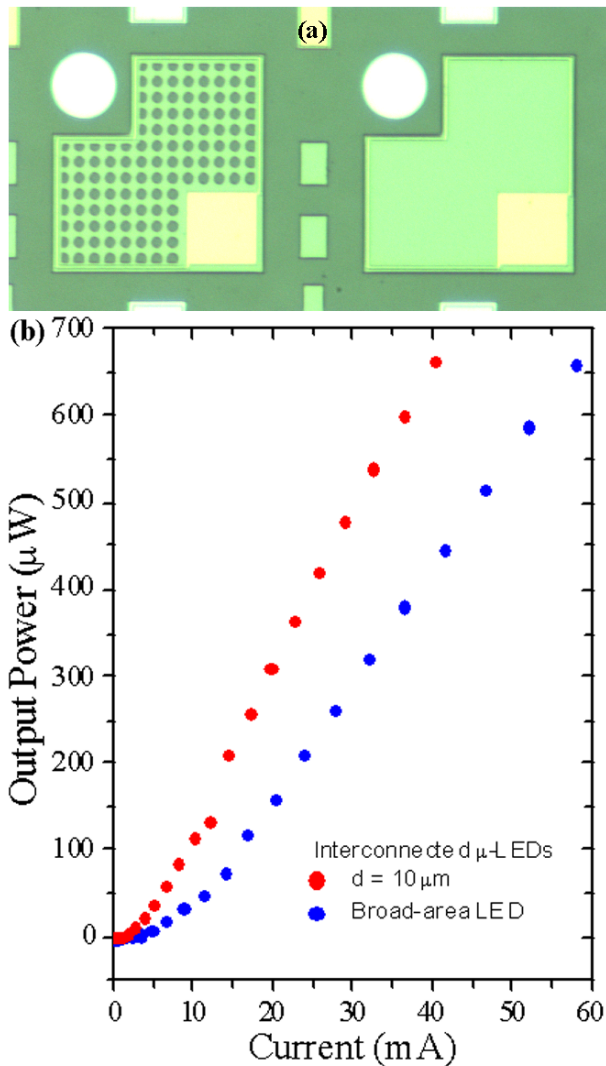


Fig. 6. Optical microscope images of a KSU conventional broad-area ( $300 \times 300 \mu\text{m}^2$ ) LED (right) and a KSU interconnected microdisk LED with individual disk diameter of  $10 \mu\text{m}$  (left) based on InGaN/GaN QWs. (b) Comparison of the L-I characteristics of an interconnected microdisk LED with disk diameter of about  $12 \mu\text{m}$  with a conventional broad-area LED measured on the top surface of unpackaged chips [after Ref. 16].

### 5. III-nitride microdisplays

We have also developed a bonding scheme that allows us to address microdisk pixels individually in an array comprising many III-nitride micro-emitters/micro-detectors. For examples, when an array such as that of Fig. 7 was forward biased and individually addressed, we have successfully demonstrated the operation of a prototype blue microdisplay [17]. The prototype device has a dimension of  $0.5 \times 0.5 \text{ mm}^2$  and consists of  $10 \times 10$  pixels of 12 microns in diameter [Fig. 7(a)]. Figure 7(b) shows optical microscope images of a blue microdisplay

in action, displaying letters “USA.” This demonstrates the operation of the first prototype semiconductor microdisplay.

The bonding scheme of these microdisplays was also utilized to characterize individual III-nitride micro-LEDs under current injection conditions. Fig. 8 shows the L-I characteristic (power output versus forward current) of three individual  $12 \mu\text{m}$  micro-LEDs within a microdisplay of Fig. 7, which demonstrated that the uniformity of light emission among these micro-LEDs is quite good. The angular distribution of light emission from these micro-LEDs has been measured through the sapphire substrate and it was seen that the escape cone for the isotropic spontaneous emission from these micro-LEDs through sapphire substrate is quite large. The result thus demonstrated that microdisplays fabricated from III-nitride QWs grown on sapphire substrates could provide a very wide viewing angle. The operating speed of these micro-LEDs has also been measured [33]. It was observed that the turn-on response was very fast (below 30 ps), while the turn-off time  $\tau_{\text{off}}$  decreased with a decrease of the m-LED size. As illustrated in Fig. 10(b),  $\tau_{\text{off}}$  decreased from 0.21 to 0.15 ns when the size was reduced from 15 to  $8 \mu\text{m}$ . This behavior is expected since the effects of surface recombination are enhanced in smaller  $\mu$ -LEDs. On the other hand, the increased operating speed may also be a result of an enhanced radiative recombination rate in micro-LEDs due to the micro-cavity effect. With this fast speed and other advantages such as long operation lifetime, III-nitride micro-LED arrays may be used to replace lasers as inexpensive short distance optical links such as between computer boards with a frequency up to 10 GHz.

Current microdisplays are based on liquid crystal dis-

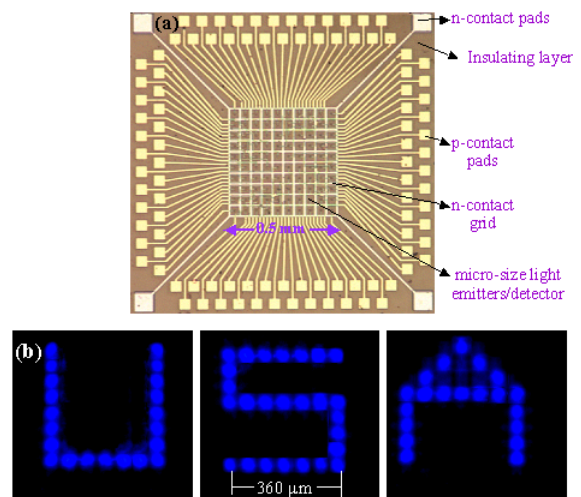


Fig. 7. (a) Optical microscope image of a bonding scheme that allows one to address each microdisk pixel individually (or a III-nitride blue microdisplay); (b) Optical microscope image of the III-nitride blue microdisplay (a) in action, displaying the letters “USA.” [after Ref. 17]

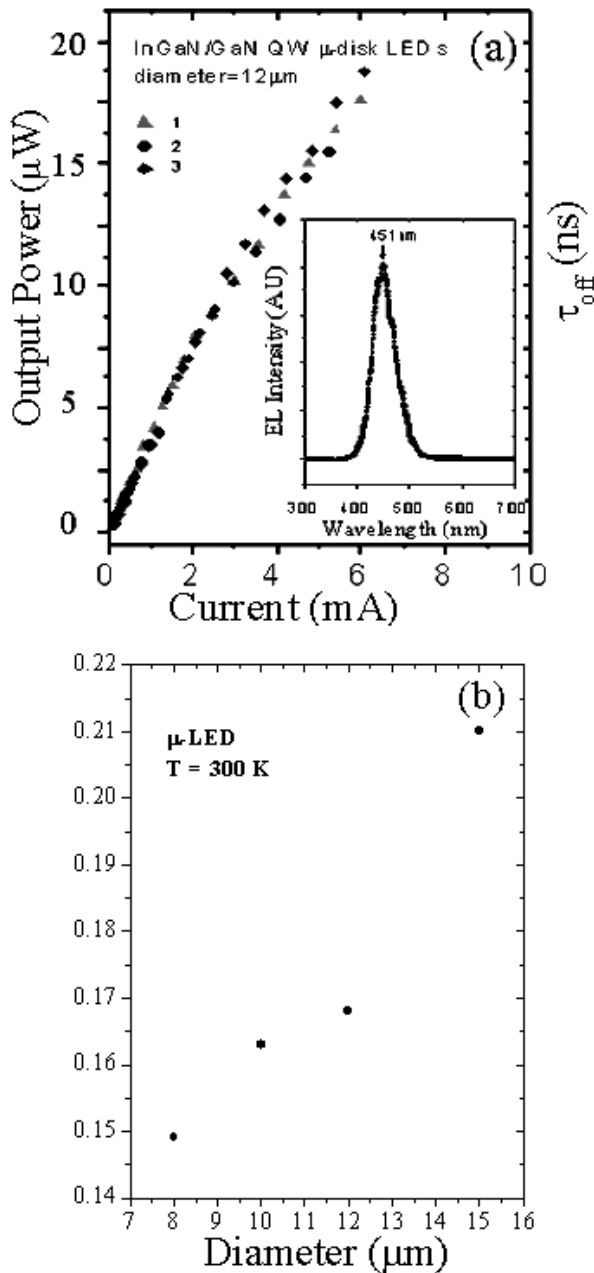


Fig. 8. (a) L-I characteristics of three individual microdisk LEDs within a microdisplay such as that in Fig. 7(a). The inset is an electroluminescent (EL) spectrum of a blue microdisk LED. The measurements were made through the sapphire substrate on unpackaged chips. (b) The size dependence of the turn-off time of the III-nitride microdisk LEDs [after Refs. 17, 33].

play technology or organic light emitting diodes. High-information content semiconductor microdisplays, which require the integration of a dense array of micro-size LEDs on a single semiconductor chip, have not been successfully fabricated. Furthermore, color conversion for full color displays cannot be achieved in conventional III-V or Si semiconductors. So far, large flat

panel displays based on semiconductor LEDs used on large buildings and stadiums are made up of a massive number of discrete LEDs. Based on the results obtained from this prototype microdisplay and the unique properties of III-nitrides, we believe that III-nitride microdisplays can potentially provide unsurpassed performance including: self-luminescent, high brightness/resolution/contrast, high temperature/high power operation, high shock resistance, wide field-of-view, full color spectrum capability, long life, high speed, and low power consumption. On the other hand, the ability of 2D array integration with advantages of high speed, high resolution, low temperature sensitivity, and applicability under versatile conditions make III-nitride micro-LEDs as a potential candidate for light sources in short distance optical communications.

#### IV. SUMMARY AND FUTURE TRENDS

We briefly summarized some of the recent advances in III-nitride microstructures and micro-size emitters made by our group. Microstructures discussed include micro-size disk, ring, and pyramid structures. Active microdisk cavity LEDs have been successfully fabricated. The results obtained so far on III-nitride micro-cavity structures and devices are very promising, as demonstrated by the examples of practical integrated device components discussed in sections 3.3 and 3.4. However, there are many problems and questions that still stand in the way of the practical device implementation for many applications based on III-nitride micro-size devices. Current injected III-nitride microcavity lasers, such as microdisk lasers, microring lasers, and vertical cavity surface emitting lasers (VCSELs) as of this writing are not yet been achieved. III-nitride integrated micro-photonics components with multiple functionalities, combining emitters, detectors, waveguides, etc. on single chips have not yet been demonstrated either.

Furthermore, the achievement of high performance micro-size LEDs operating in the ultraviolet spectral regions with wavelengths shorter than 340 nm will allow chip-scale integration of Chem/Bio sensors for detection of chemical or biological threats. Other applications include pre-cancer cells detection with compact UV source in medical and health care. Protein fluorescence is generally excited by UV light sources and changes in intrinsic fluorescence can be used to monitor structural changes in a protein. The availability of chip-scale UV light sources may open new avenues for medical research. However, these devices require the use of high quality and highly conductive  $\text{Al}_x\text{Ga}_{1-x}\text{N}$  or  $\text{In}_x\text{Al}_y\text{Ga}_{1-x-y}\text{N}$  alloys with high Al contents. P-type conductive AlGaN alloys with relatively high Al contents are indispensable for hole injection for many photonics devices that are active in the UV spectral region, which remains one of the foremost challenging tasks of the Nitride community. At the same

time, novel approaches for micro-size ohmic contact fabrication, p-type contacts in particular, must be further developed to curtail the problem of relatively low p-type conductivity in III-nitrides. Finally, wavelength scale III-nitride photonic devices are also to be explored.

It is our belief that III-nitride micro-photonics are expected to possess special functionalities in the visible and UV spectral regions and open many important applications in areas such as communications, signal and image processing, energy conversion and storage, chemical-bio-hazard substance and disease detection. Nevertheless, further understanding of fundamental properties is required and novel growth methods to further reduce defects and novel device structural designs must be explored in order for their potential to become a reality.

### ACKNOWLEDGMENTS

The work is supported by ARO, NSF (DMR-9902431, and DMR-0203373), ONR, DOE (96ER45604/A000). We would like to acknowledge the contributions of the following current and former members of our group: Dr. R. Mair, Dr. K. C. Zeng, Dr. L. Dai, Visiting Prof. S. X. Jin, J. Li, J. Shakya, K. H. Kim, M. L. Nakarmi, K. B. Nam, Dr. T. N. Order, and W. P. Zhao.

### REFERENCES

- [1] H. Morkoc, S. Strite, G. B. Gao, M. E. Lin, B. Sverdlov and M. Burns, *J. Appl. Phys.* **76**, 1363 (1994).
- [2] S. Nakamura, T. Mukai and M. Senoh, *Appl. Phys. Lett.* **64**, 1687 (1994).
- [3] M. Asif Khan, M. S. Shur, J. N. Kuznia, Q. Chen, J. Burn and W. Schaff, *Appl. Phys. Lett.* **66**, 1083 (1995).
- [4] S. N. Mohammad, Z.-F. Fan, A. Salvador, O. Aktas, A. E. Botchkarev, W. Kim and H. Morkoc, *Appl. Phys. Lett.* **69**, 1420 (1996).
- [5] S. Nakamura, M. Senoh, N. Iwasa and S. Nagahama, *Jpn. J. Appl. Phys.* **34**, L797 (1995).
- [6] *Nitride News, Compound Semiconductor* **3**, 4 (1997).
- [7] R. K. Chang and A. J. Campillo, *Optical Processes in Microcavities* (World Scientific, Singapore, 1996).
- [8] Y. Yamamoto and R. E. Slusher, *Physics Today* **46**, 66 (1993).
- [9] R. A. Mair, K. C. Zeng, J. Y. Lin, H. X. Jiang, B. Zhang, L. Dai, H. Tang, A. Botchkarev, W. Kim and H. Morkoc, *Appl. Phys. Lett.* **71**, 2898 (1997).
- [10] R. A. Mair, K. C. Zeng, J. Y. Lin, H. X. Jiang, B. Zhang, L. Dai, A. Botchkarev, W. Kim, H. Morkoc and M. A. Khan, *Appl. Phys. Lett.* **72**, 1530 (1998).
- [11] R. Mair, K. C. Zeng, J. Y. Lin, H. X. Jiang, B. Zhang, L. Dai, H. Tang, W. Kim, A. Botchkarev, H. Morkoc and M. Asif Khan, *Symposium Proceedings of Materials Research Society* **482**, 649 (1998).
- [12] K. C. Zeng, L. Dai, J. Y. Lin and H. X. Jiang, *Appl. Phys. Lett.* **75**, 2563 (1999).
- [13] K. C. Zeng, J. Y. Lin, H. X. Jiang and W. Yang, *Appl. Phys. Lett.* **74**, 1227 (1999).
- [14] H. X. Jiang, J. Y. Lin, K. C. Zeng and W. Yang, *Appl. Phys. Lett.* **75**, 763 (1999).
- [15] S. X. Jin, J. Li, J. Y. Lin and H. X. Jiang, *Appl. Phys. Lett.* **76**, 631 (2000).
- [16] S. X. Jin, J. Li, J. Y. Lin and H. X. Jiang, *Appl. Phys. Lett.* **77**, 3236 (2000).
- [17] H. X. Jiang, S. X. Jin, J. Li, J. Shakya and J. Y. Lin, *Appl. Phys. Lett.* **78**, 1303 (2001).
- [18] <http://www.phys.ksu.edu/area/GaNgroup>.
- [19] N. C. Frateschi, A. P. Kanjamala and A. F. J. Levi, *Appl. Phys. Lett.* **66**, 1859 (1995).
- [20] N. C. Frateschi and A. F. J. Levi, *J. Appl. Phys.* **80**, 644 (1996).
- [21] R. P. Wang and M. M. Dumitrescu, *J. Appl. Phys.* **81**, 3391 (1997).
- [22] *Lord Rayleigh, in Scientific Papers*, (Cambridge University, Cambridge, 1912), Vol. 5, p. 617.
- [23] *Numerical Data and Functional Relationships in Science and Technology*, edited by P. Eckerlin and H. Kandler (Springer, Berlin, Landolt-Bornstein, 1971), Vol. III.
- [24] Y. Kawabe, Ch. Spiegelberg, A. Schulzgen, M. F. Nabor, B. Kippelen, E. A. Mash, P. M. Allemand, M. Kuwata-Gonokami, K. Takeda and N. Pryghambarian, *Appl. Phys. Lett.* **72**, 141 (1998).
- [25] R. Underwood, D. Kopolnek, B. Keller, S. DenBaars and U. Mishra, *Topical Workshop on Nitrides* (Nagoya, Sep., 1995).
- [26] T. S. Zheleva, O. H. Nam, M. D. Bremser and R. F. Davis, *Appl. Phys. Lett.* **71**, 2472 (1997).
- [27] T. Akasaka, Y. Kobayashi, A. Ando and N. Kobayashi, *Appl. Phys. Lett.* **71**, 2196 (1997).
- [28] B. Beaumont, S. Haffouz and P. Gibart, *Appl. Phys. Lett.* **72**, 921 (1998).
- [29] S. Bidnyk, B. D. Little, Y. H. Cho, J. Karasinski, J. J. Song, W. Yang and S. A. McPherson, *Appl. Phys. Lett.* **73**, 2242 (1998).
- [30] K. C. Zeng, J. Y. Lin, H. X. Jiang and W. Yang, *Appl. Phys. Lett.* **74**, 1227 (1999).
- [31] K. Tachibana, T. Someya, A. Ishida and Y. Arakawa, *Appl. Phys. Lett.* **76**, 3212 (2000).
- [32] S. Bidnyk, B. D. Little, Y. H. Cho, J. Karasinski, J. J. Song, W. Yang and S. A. McPherson, *Appl. Phys. Lett.* **73**, 2242 (1998).
- [33] S. X. Jin, J. Li, J. Shakya, J. Y. Lin and H. X. Jiang, *Appl. Phys. Lett.* **78**, 3532 (2001).